

**CHAPTER VI**  
**ACTIVITY OF Pt/CeO<sub>2</sub>, Au/CeO<sub>2</sub>, Au/Fe<sub>2</sub>O<sub>3</sub>, Pt/CeO<sub>2</sub>.Al<sub>2</sub>O<sub>3</sub>,  
Au/CeO<sub>2</sub>.Al<sub>2</sub>O<sub>3</sub> AND Au/Fe<sub>2</sub>O<sub>3</sub>.Al<sub>2</sub>O<sub>3</sub> CATALYSTS :**  
**FOR WATER GAS SHIFT REACTION**

In our previous studies on selective CO oxidation over a reaction temperature range of 50-360°C, we found that the Pt/CeO<sub>2</sub> sol-gel, Au/CeO<sub>2</sub> co-precipitation catalysts exhibited high activity and selectivity. In this chapter, the results of the catalytic activity of the Pt/CeO<sub>2</sub>, Au/CeO<sub>2</sub> and Au/Fe<sub>2</sub>O<sub>3</sub> catalysts for low temperature water gas shift (WGS) reaction with no H<sub>2</sub> presence presented. The activity of these catalysts was tested with a flow reactor using a reactant mixture composition of 4% CO, 2.6-20% H<sub>2</sub>O and helium in the low temperature range of 120-360°C.

As alumina is the support most widely used in metal-supported catalysts and because of its importance, alumina is the support largely used in gas exhaust catalytic converters. Therefore, we also present the results of our efforts to increase the activity and also increase the stability of these catalysts for WGSR by modification of the CeO<sub>2</sub> or Fe<sub>2</sub>O<sub>3</sub> support with high surface area Al<sub>2</sub>O<sub>3</sub>. The activity of these catalysts was tested in a reactor using a reactant mixture composition of 1% CO, 20% H<sub>2</sub>O, 40% H<sub>2</sub> and helium in the low temperature range of 120-360°C.

The H<sub>2</sub> was added because the aim is to investigate their activity in WGSR for fuel cell applications by allowing the syngas to react with steam with a typical catalyst.. BET, XRD, and SEM analyses of the samples give additional information on the morphological structure of investigated samples.

## **6.1 Experimental Details**

### **6.1.1 Catalyst Preparation**

The 1% Pt/CeO<sub>2</sub> catalyst was synthesized using the sol-gel method. The single step sol-gel catalyst was prepared by hydrolyzing a solution of Ce acetate and H<sub>2</sub>PtCl<sub>6</sub>.6H<sub>2</sub>O with NH<sub>4</sub>OH. The reaction mixture was aged at 80°C and pH of

9.0 to 9.5 for an hour. Then,  $\text{HNO}_3$  was added until gelation. The catalysts were dried overnight at  $110^\circ\text{C}$  and calcined at  $500^\circ\text{C}$  for 5 h.

The 1%  $\text{Au/CeO}_2$  catalyst was prepared using the co-precipitation from a mixture of  $\text{HAuCl}_4 \cdot 3\text{H}_2\text{O}$ ,  $\text{Ce}(\text{NO}_3)_3 \cdot 6\text{H}_2\text{O}$  and  $\text{Na}_2\text{CO}_3$  solution at room temperature and constant pH of 8.0. The precipitate was aged for an hour at room temperature. The precipitate was then filtered and washed with deionized water until there were no anions detectable in the wash. After washing, the catalysts were dried overnight at  $110^\circ\text{C}$  and calcined in air at  $500^\circ\text{C}$  for 5 h.

In the case of 3%  $\text{Au/Fe}_2\text{O}_3$  catalysts, they were prepared using co-precipitation and deposition-precipitation methods (Andreeva *et al.*, 1996). For the co-precipitation method,  $\text{Fe}(\text{NO}_3)_3 \cdot 6\text{H}_2\text{O}$  was used as a precursor.

The deposition-precipitation catalyst was prepared by deposition of gold hydroxide with a solution of  $\text{Na}_2\text{CO}_3$  at  $60^\circ\text{C}$  and pH of 8. The precipitate was aged for 1 h, filtered and washed carefully until absence of excess anions. Then, samples were dried at  $110^\circ\text{C}$  and calcined at  $400^\circ\text{C}$  for 2 h.

The 1%  $\text{Pt/CeO}_2 \cdot \text{Al}_2\text{O}_3$  catalyst was synthesized using impregnation method. The catalysts were prepared by impregnation of  $\text{Al}_2\text{O}_3$  sol-gel support with aqueous solutions of  $\text{Ce}(\text{NO}_3)_3$  for  $\text{CeO}_2$  and  $\text{H}_2\text{PtCl}_6$  for Pt. The  $\text{Pt/CeO}_2 \cdot \text{Al}_2\text{O}_3$  catalyst was prepared by successive impregnations, of  $\text{CeO}_2$  first, followed by the impregnation of Pt.

For 1%  $\text{Au/CeO}_2 \cdot \text{Al}_2\text{O}_3$  catalyst,  $\text{HAuCl}_4 \cdot 3\text{H}_2\text{O}$  was used as a precursor. In the case of 1%  $\text{Au/Fe}_2\text{O}_3 \cdot \text{Al}_2\text{O}_3$  catalysts, they were prepared using deposition-precipitation methods and  $\text{Fe}(\text{NO}_3)_3 \cdot 6\text{H}_2\text{O}$  was used as a precursor. The samples were dried at  $110^\circ\text{C}$  and calcined at  $400^\circ\text{C}$  for 2 h and  $500^\circ\text{C}$  for 5 h.

### 6.1.2 Catalyst Characterization

Powder X-ray diffraction (XRD) patterns were collected in air on a Rigaku Powder Diffractometer using  $\text{CuK}\alpha$  radiation with a nickel filter. The BET surface area of the samples was analyzed by nitrogen adsorption with an Autosorb automated gas sorption analyzer. Scanning electron microscope (SEM) measurements were performed by using JEOL JSM-5410LV scanning microscope

operated at 15 kV. The transmission electron microscopy (TEM) was carried out using a JEM 2010 operating at 200 kV in bright and dark field modes. Crystallinity and crystal structure of the sample were evaluated from selected area electron diffraction pattern.

### 6.1.3 Catalytic Testing

The catalytic activity tests of the catalysts in the WGS reaction were carried out at atmospheric pressure and in the temperature range of 120-360°C in a U-tube pyrex reactor having an internal diameter of 6 mm. The catalysts were tested for their activities in a gas mixture typically containing 4% CO in He, saturated with water vapor. The temperature of the gas bubbler was controlled in order to obtain variable H<sub>2</sub>O/CO ratio. The space velocity was 30,000 ml/g h. The 1% Pt/CeO<sub>2</sub>, 1% Au/CeO<sub>2</sub>, 1% Pt/CeO<sub>2</sub>.Al<sub>2</sub>O<sub>3</sub> and 1% Au/CeO<sub>2</sub>.Al<sub>2</sub>O<sub>3</sub> catalysts were pretreated at 110°C for 2 h in the O<sub>2</sub> atmosphere. In the case of 3%Au/Fe<sub>2</sub>O<sub>3</sub> and 3%Au/Fe<sub>2</sub>O<sub>3</sub>.Al<sub>2</sub>O<sub>3</sub> catalysts, the reduction of the sample was conducted at 250°C for 12 h in a H<sub>2</sub>/He mixture (1%H<sub>2</sub>). The reactant and product composition was analyzed by a gas chromatograph (GC) equipped with a thermal conductivity detector (TCD) and a 10 ft x 1/8 inch stainless steel packed column filled with carbosphere.

## 6.2 Results and Discussion

### 6.2.1 Catalyst Characterization

The measured data of the BET surface areas of samples are listed in Table 6.1. The BET surface areas of the 1% Pt/CeO<sub>2</sub> sol-gel, 1% Au/CeO<sub>2</sub> co-precipitation, and 3% Au/Fe<sub>2</sub>O<sub>3</sub> co-precipitation and deposition-precipitation catalysts are 55.0, 124.1, 345.0, and 79.5 m<sup>2</sup>/g, respectively. The results indicate that the surface area is dependent on the catalyst preparation method and catalyst type. In addition, it was observed that the surface area of 3% Au/Fe<sub>2</sub>O<sub>3</sub> deposition-precipitation catalyst was slightly higher than that reported in the literature, which is about 66.5 m<sup>2</sup>/g (Andreeva *et al.*, 1998).

**Table 6.1** Surface area of 1% Pt/CeO<sub>2</sub>, 1% Au/CeO<sub>2</sub>, 3% Au/Fe<sub>2</sub>O<sub>3</sub> catalysts.

Catalyst	Preparation method	BET surface area (m <sup>2</sup> /g)
1% Pt/CeO <sub>2</sub>	Sol-gel	55.0
1% Au/CeO <sub>2</sub>	Co-precipitation	124.1
3% Au/Fe <sub>2</sub> O <sub>3</sub>	Co-precipitation	345.0
3% Au/Fe <sub>2</sub> O <sub>3</sub>	Deposition-precipitation	79.5

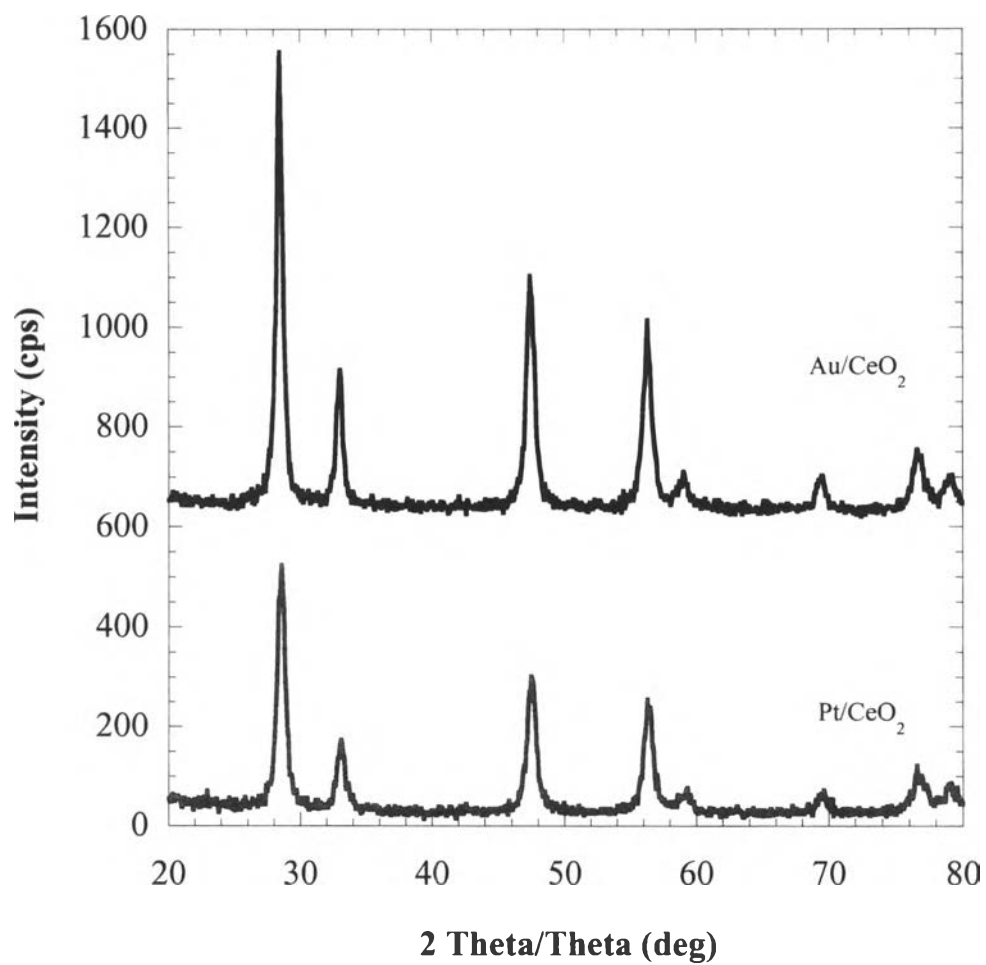
The measured data of the BET surface areas of samples are listed in Table 6.2. The BET surface areas of the 1% Pt/CeO<sub>2</sub>.Al<sub>2</sub>O<sub>3</sub>, 1% Au/CeO<sub>2</sub>.Al<sub>2</sub>O<sub>3</sub>, and 3% Au/Fe<sub>2</sub>O<sub>3</sub>.Al<sub>2</sub>O<sub>3</sub> catalysts are 281.5, 284.0, and 357.7 m<sup>2</sup>/g, respectively. The BET surface area of the sample on amorphous iron oxide was the largest in comparison with the other studied samples.

**Table 6.2** Surface area of 1% Pt/CeO<sub>2</sub>.Al<sub>2</sub>O<sub>3</sub>, 1% Au/CeO<sub>2</sub>.Al<sub>2</sub>O<sub>3</sub>, and 3% Au/Fe<sub>2</sub>O<sub>3</sub>.Al<sub>2</sub>O<sub>3</sub> catalysts.

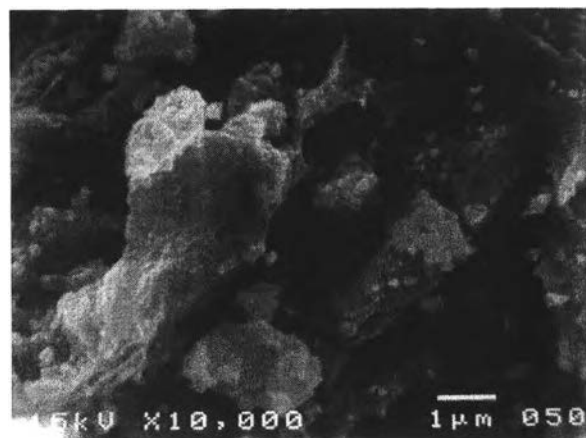
Catalyst	Preparation method	BET surface area (m <sup>2</sup> /g)	Average pore size (Å)
1% Pt/CeO <sub>2</sub> .Al <sub>2</sub> O <sub>3</sub>	Impregnation	281.5	78.94
1% Au/CeO <sub>2</sub> .Al <sub>2</sub> O <sub>3</sub>	Impregnation	284.0	81.90
3% Au/Fe <sub>2</sub> O <sub>3</sub> .Al <sub>2</sub> O <sub>3</sub>	Deposition-precipitation	357.7	71.48
Al <sub>2</sub> O <sub>3</sub>	Sol-gel	348.4	82.69

Figure 6.1 shows the comparison of XRD patterns of Pt/CeO<sub>2</sub> and Au/CeO<sub>2</sub> catalysts. No evidence of metallic peaks was observed and it can be concluded that the average crystallite sizes of metals for both catalysts were smaller than 5 nm. The crystallite sizes of ceria were determined from X-ray line-broadening using the Debye Scherrer equation. This figure also shows that the ceria support is highly crystalline with an approximate crystallite size of 34.8 and 14.5 nm for Pt/CeO<sub>2</sub> and Au/CeO<sub>2</sub> catalysts, respectively. In contrast, the sample of Au/Fe<sub>2</sub>O<sub>3</sub> shows diffraction patterns which mainly correspond to amorphous ferrihydrite or comprise the poorly crystalline phases of ferrihydrite and  $\alpha$ -Fe<sub>2</sub>O<sub>3</sub> (hematite).

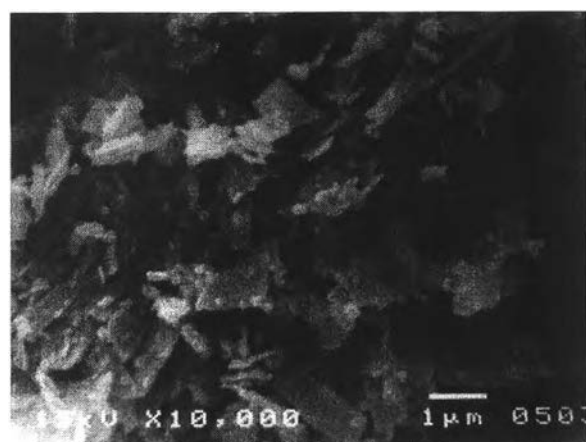
The morphological differences between the catalysts were observed by SEM which are shown in Figure 6.2. The Pt/CeO<sub>2</sub> sol-gel catalyst shows a porous morphology. Au/CeO<sub>2</sub> co-precipitation catalyst is in the form of highly crystalline flakes and Au/Fe<sub>2</sub>O<sub>3</sub> deposition-precipitation catalyst is amorphous and appears to consist of non porous aggregates of primary spherical particles of  $\sim 1000$  Å diameter. The SEM pattern of Au/CeO<sub>2</sub> catalyst is confirmed by the XRD result, which shows that the crystallinity of CeO<sub>2</sub> in this catalyst is higher than that of Pt/CeO<sub>2</sub> catalyst and amorphous patterns of Au/Fe<sub>2</sub>O<sub>3</sub> catalyst.



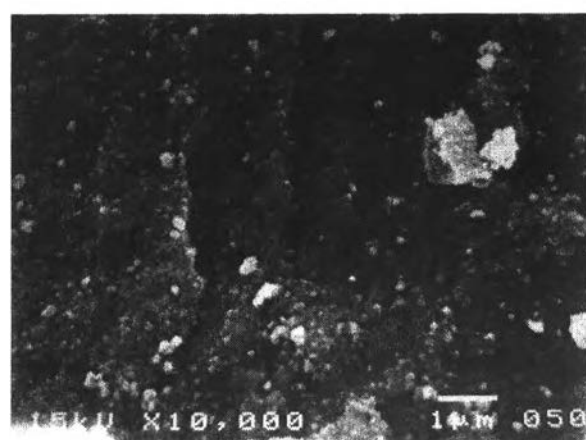
**Figure 6.1** XRD patterns obtained from the 1% Pt/CeO<sub>2</sub> sol-gel and 1% Au/CeO<sub>2</sub> co-precipitation catalysts.



(a)



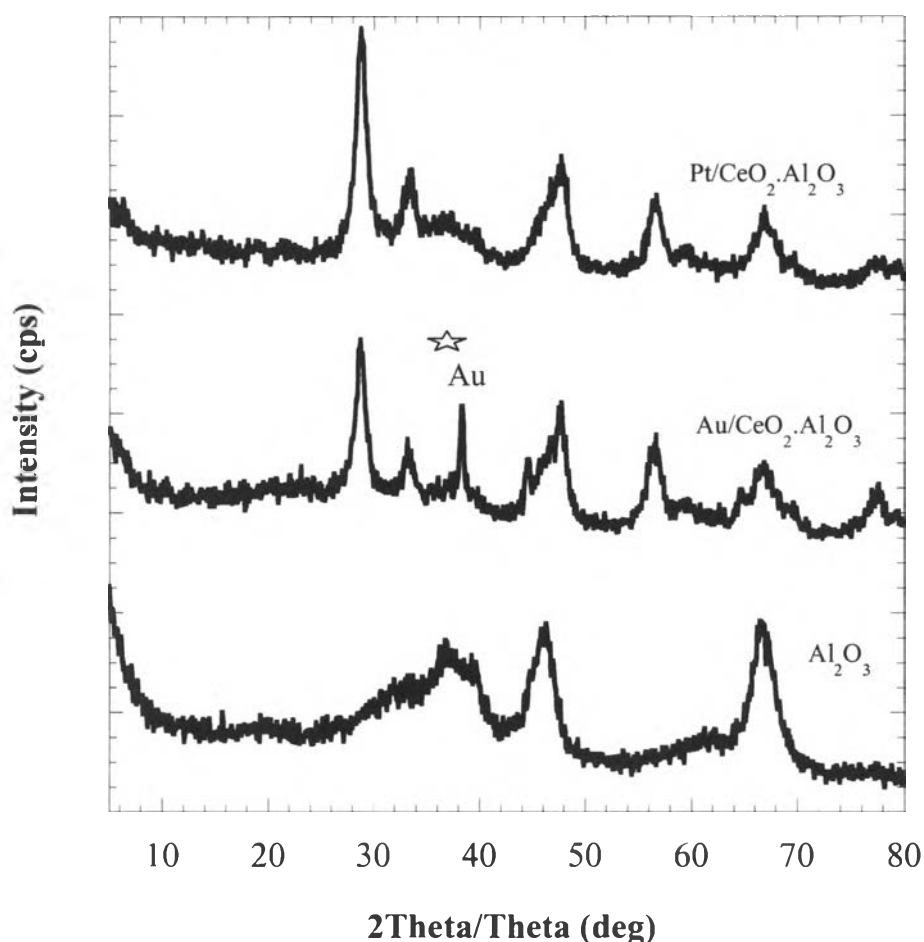
(b)



(c)

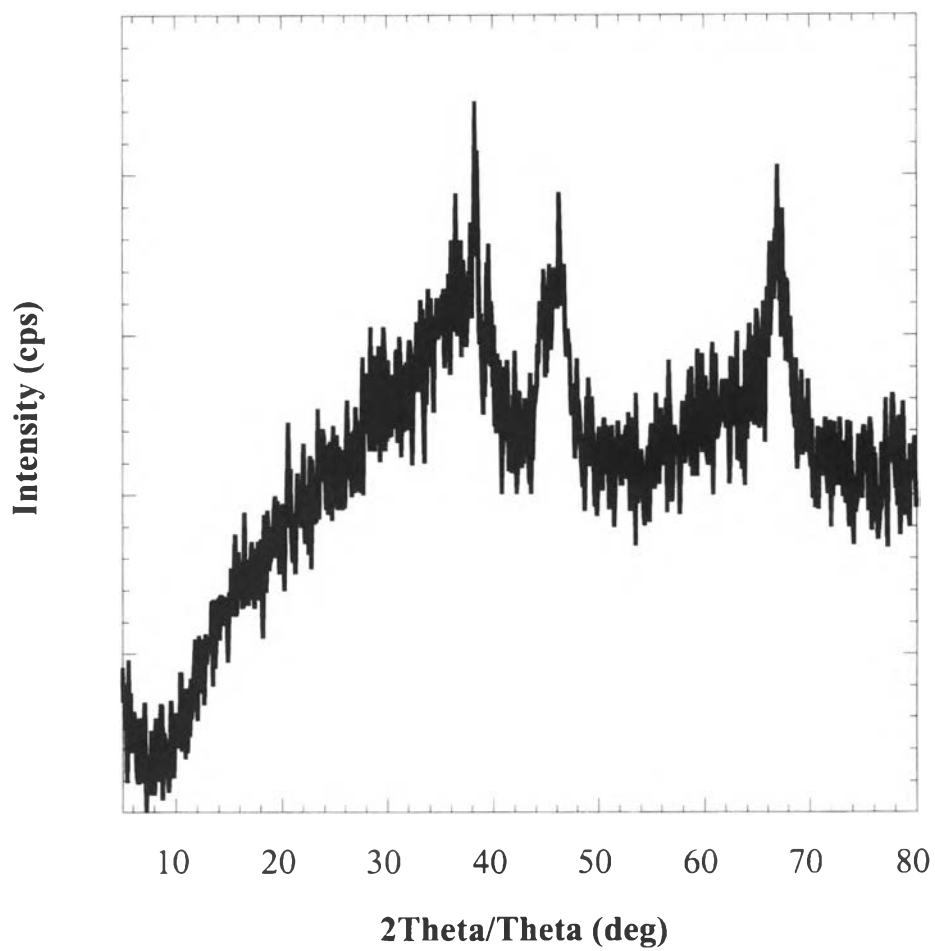
**Figure 6.2** SEM photographs of (a) 1% Pt/CeO<sub>2</sub>; (b) 1% Au/CeO<sub>2</sub>; (c) 3% Au/Fe<sub>2</sub>O<sub>3</sub> catalysts.

Figure 6.3 shows the comparison of XRD patterns of 1% Pt/CeO<sub>2</sub>.Al<sub>2</sub>O<sub>3</sub>, 1% Au/CeO<sub>2</sub>.Al<sub>2</sub>O<sub>3</sub>, and 3% Au/Fe<sub>2</sub>O<sub>3</sub>.Al<sub>2</sub>O<sub>3</sub> catalysts. This figure also shows that XRD patterns of the 1% Pt/CeO<sub>2</sub>.Al<sub>2</sub>O<sub>3</sub> and 1% Au/CeO<sub>2</sub>.Al<sub>2</sub>O<sub>3</sub> catalyst did not change the pattern of CeO<sub>2</sub> and Al<sub>2</sub>O<sub>3</sub> support significantly. However, for Au/CeO<sub>2</sub>.Al<sub>2</sub>O<sub>3</sub> catalysts, the Au (111) peak was found at ~38.2° (2θ). The XRD pattern of Au/Fe<sub>2</sub>O<sub>3</sub>.Al<sub>2</sub>O<sub>3</sub> catalyst is shown in Figure 6.4 which shows Au peak at ~38.2° (2θ), α-Fe<sub>2</sub>O<sub>3</sub> phase at ~35.6° (2θ) and Al<sub>2</sub>O<sub>3</sub> peak at ~46.0 and 67.0° (2θ).



**Figure 6.3** XRD patterns obtained from the 1% Pt/CeO<sub>2</sub>.Al<sub>2</sub>O<sub>3</sub>, 1% Au/CeO<sub>2</sub>.Al<sub>2</sub>O<sub>3</sub> catalysts, and Al<sub>2</sub>O<sub>3</sub> support.





**Figure 6.4** XRD pattern obtained from 3% Au/Fe<sub>2</sub>O<sub>3</sub>.Al<sub>2</sub>O<sub>3</sub> catalyst.

### 6.2.2 Catalytic Activity

The catalytic activity of Pt/CeO<sub>2</sub>, Au/CeO<sub>2</sub> and Au/Fe<sub>2</sub>O<sub>3</sub> catalysts was examined in this work. The catalytic activity expressed as the percentage of the CO conversion in the WGS reaction versus reaction temperature was carried out with a feed stream typically consisting of 4% CO, 2.6% H<sub>2</sub>O and helium. The results are shown in Figure 6.5. The sequence of the catalysts arranged for decreasing activity is the following. Au/Fe<sub>2</sub>O<sub>3</sub> (deposition precipitation) > Pt/CeO<sub>2</sub> > Au/CeO<sub>2</sub> > Au/Fe<sub>2</sub>O<sub>3</sub> (co-precipitation).

The Au/Fe<sub>2</sub>O<sub>3</sub> deposition-precipitation catalyst is very active in comparison to all other catalysts examined and reached a maximum CO conversion of 34% at 320°C. However, the result of Au/Fe<sub>2</sub>O<sub>3</sub> presented in this work gave much lower activity than in the literature. Andreeva *et al.* (1996) have proposed the associative mechanism for the WGS reaction and attributed the catalytic activity to the ability of Au atoms to generate hydroxyl groups. The lowest activity is shown by highly crystalline CeO<sub>2</sub> containing Au/CeO<sub>2</sub> catalyst. This catalyst gave a maximum conversion of 9% at 320°C. It is clearly seen that the activity of the catalysts is related to the kind of support used and there is no correlation between the activity and the surface area. Our results are in agreement with Basinka *et al.* (1999) who studied the effect of support on WGS activity of Ru catalysts. It can be seen from SEM result that Au/Fe<sub>2</sub>O<sub>3</sub> is in amorphous form. This result disagrees with Tabakova *et al.* (2000) who observed that the lowest catalytic activity is shown by the amorphous and poorly crystallized catalyst.

Interestingly, when comparing the effect of preparation method on Au/Fe<sub>2</sub>O<sub>3</sub> catalysts, it was found that deposition-precipitation gave higher CO conversion than co-precipitation. This has been explained by Andreeva *et al.* (1998) as deposition-precipitation method giving a weaker interaction between gold particles and the support making it more favorable for catalysis. In contrast, co-precipitation method gave gold cluster formation which became inaccessible to catalysis.

Basinka *et al.* (1999) described that mean size of particles of metallic Ru is the most important influence on the catalyst activity. In this work, the mean size of particle of metallic catalysts is not observed by XRD and TEM. No obvious

correlation was observed between the size of Au or Pt crystallites and the catalyst activity.

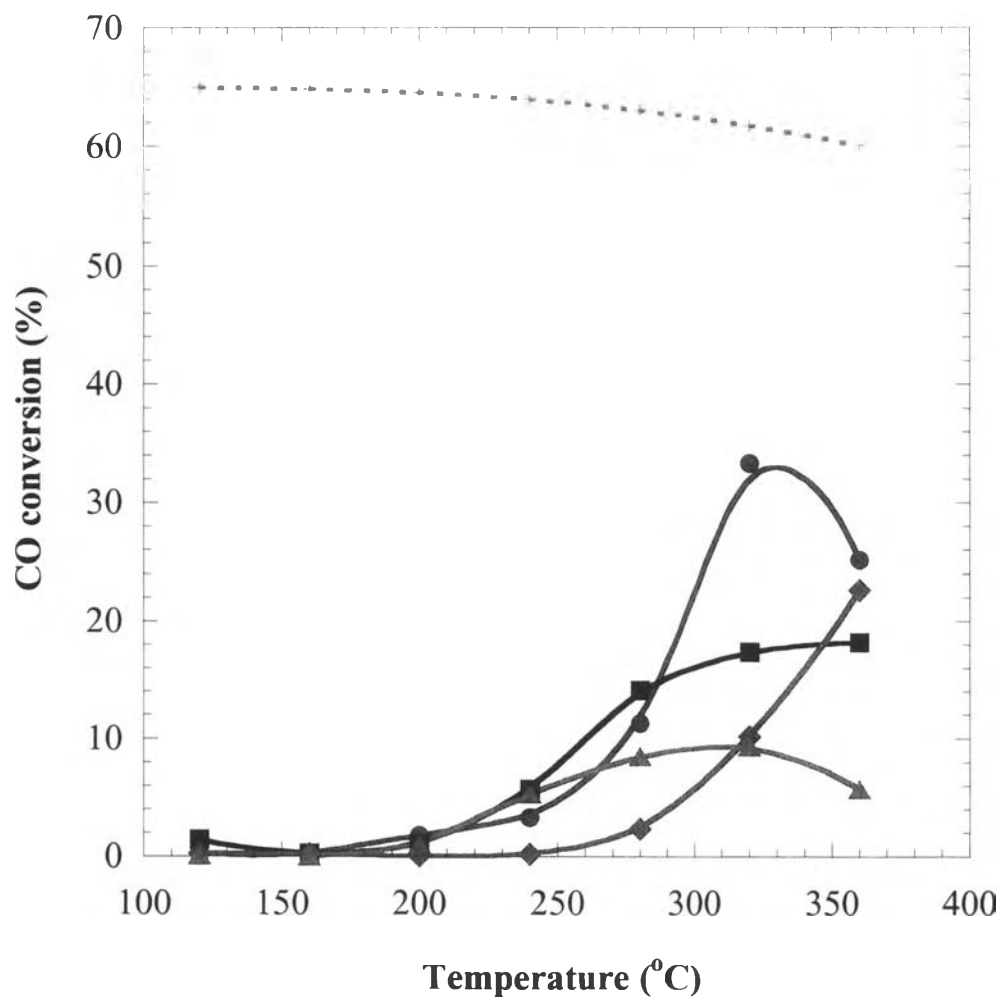


**Figure 6.5** Temperature dependence of WGS activity of the catalysts studied; (■) 1% Pt/CeO<sub>2</sub> sol-gel; (◆) 1% Au/CeO<sub>2</sub> co-precipitation; (●) 3% Au/Fe<sub>2</sub>O<sub>3</sub> deposition-precipitation; (▲) 3% Au/Fe<sub>2</sub>O<sub>3</sub> co-precipitation; (---) Thermodynamic equilibrium.

It is mentioned previously that the catalysts were prepared by impregnation on high surface area of  $\text{Al}_2\text{O}_3$ . Therefore, a series of experiments were performed to determine the effect of temperature and  $\text{H}_2$  concentration on  $\text{H}_2$  production from CO on  $\text{Pt/CeO}_2\cdot\text{Al}_2\text{O}_3$ ,  $\text{Au/CeO}_2\cdot\text{Al}_2\text{O}_3$ ,  $\text{Au/Fe}_2\text{O}_3\cdot\text{Al}_2\text{O}_3$ . The results are shown in Figures 6.6-6.7. The  $\text{Pt/CeO}_2\cdot\text{Al}_2\text{O}_3$  catalyst is the most active in comparison to all other catalysts examined and reached a maximum CO conversion of 54% at  $360^\circ\text{C}$ . The lowest activity is shown by  $\text{Au/CeO}_2\cdot\text{Al}_2\text{O}_3$  catalyst. This catalyst gave a maximum conversion of 6% at  $360^\circ\text{C}$ .

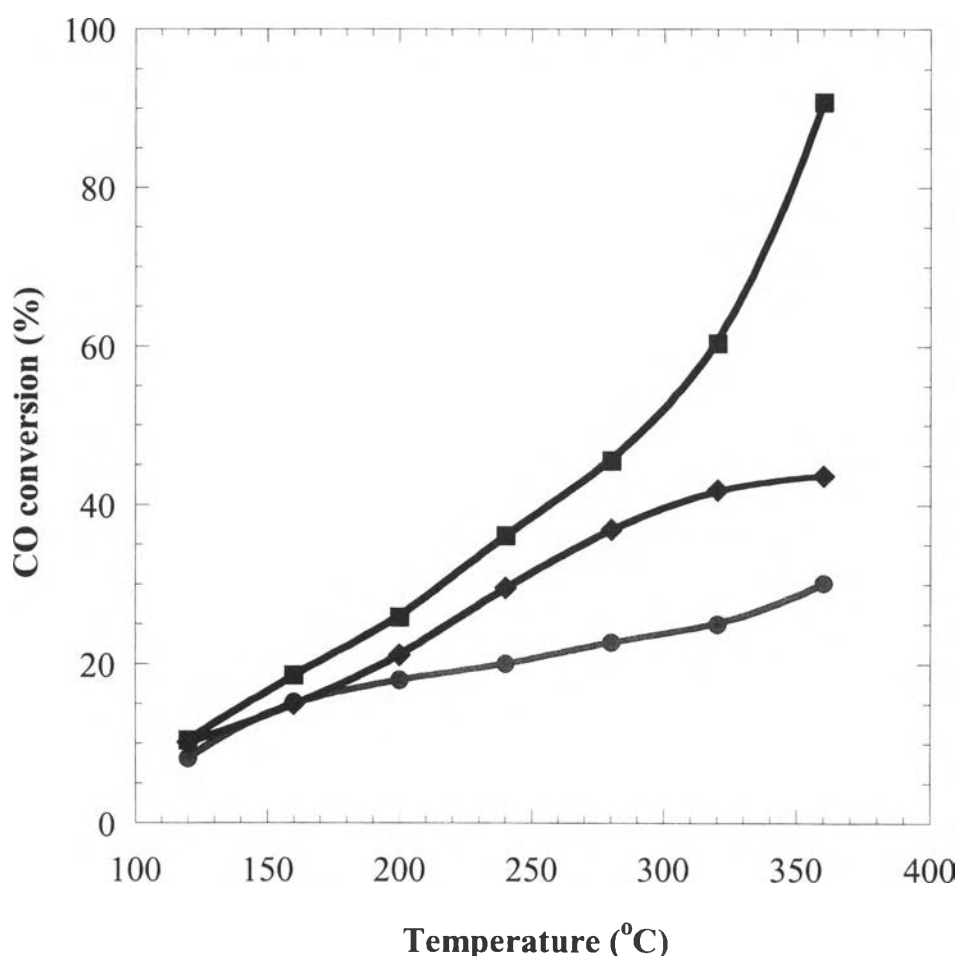


**Figure 6.6** The catalytic activity of 1%  $\text{Pt/CeO}_2\cdot\text{Al}_2\text{O}_3$ , 1%  $\text{Au/CeO}_2\cdot\text{Al}_2\text{O}_3$ , and 3%  $\text{Au/Fe}_2\text{O}_3\cdot\text{Al}_2\text{O}_3$  catalysts. Reactant composition: 1% CO, 20%  $\text{H}_2\text{O}$ , and He; (■) 1%  $\text{Pt/CeO}_2\cdot\text{Al}_2\text{O}_3$ ; (●) 1%  $\text{Au/CeO}_2\cdot\text{Al}_2\text{O}_3$ ; (◆) 3%  $\text{Au/Fe}_2\text{O}_3\cdot\text{Al}_2\text{O}_3$ .

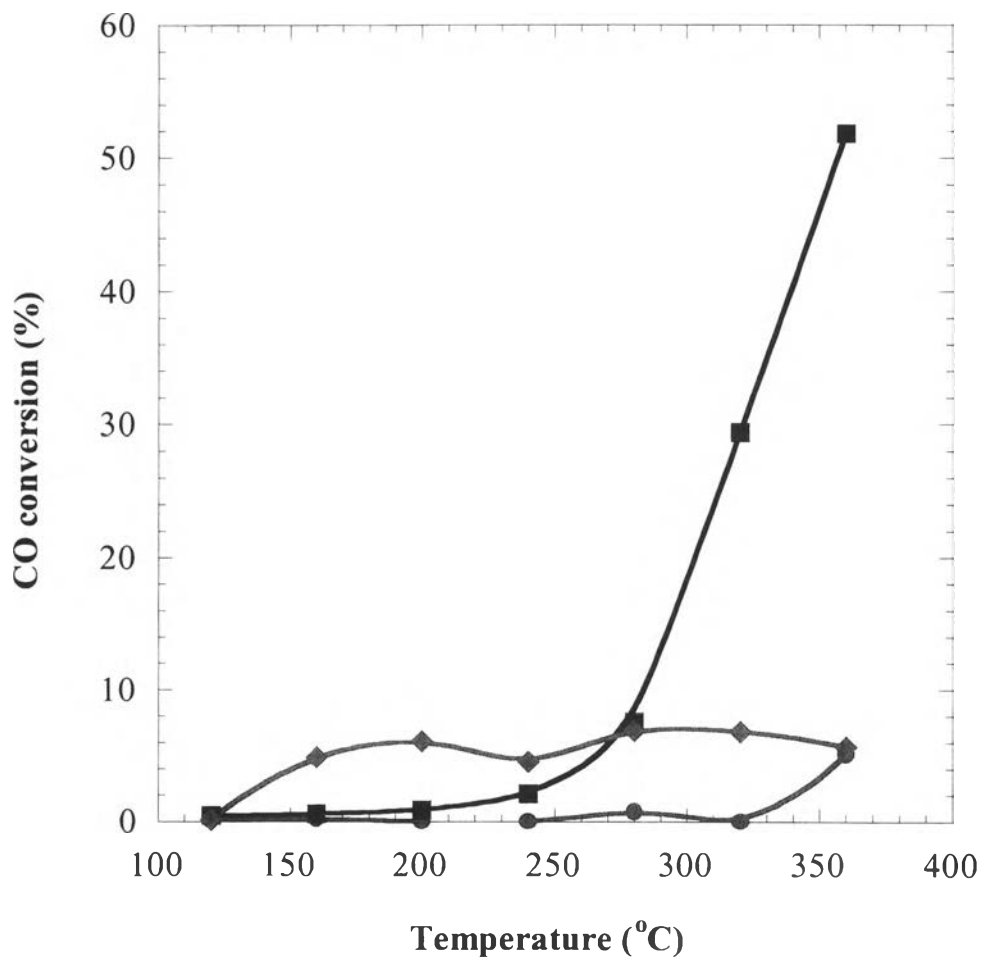


**Figure 6.7** The catalytic activity of 1% Pt/CeO<sub>2</sub>.Al<sub>2</sub>O<sub>3</sub>, 1% Au/CeO<sub>2</sub>.Al<sub>2</sub>O<sub>3</sub>, and 3% Au/Fe<sub>2</sub>O<sub>3</sub>.Al<sub>2</sub>O<sub>3</sub> catalysts. Reactant composition: 1% CO, 20% H<sub>2</sub>O, 40% H<sub>2</sub> and He; (■) 1% Pt/CeO<sub>2</sub>.Al<sub>2</sub>O<sub>3</sub>; (●) 1% Au/CeO<sub>2</sub>.Al<sub>2</sub>O<sub>3</sub>; (◆) 3% Au/Fe<sub>2</sub>O<sub>3</sub>.Al<sub>2</sub>O<sub>3</sub>.

### 6.2.3 Effect of Water Vapor

Water gas shift reaction is a reversible, exothermic reaction that is thermodynamically unfavorable at elevated temperatures. In order to achieve high conversion, additionally excess steam is used to drive the reaction thermodynamically. We tested the dependence of activity on water vapor concentration by increasing the water vapor in the feed stream from 2.6% to 20%. The results are shown in Figures 6.8-6.10. It is clearly seen from Figure 6.8 that the water vapor content significantly enhanced the catalytic performance of Pt/CeO<sub>2</sub> catalyst in the temperature range of 200-360°C. The maximum CO conversion increased from 18% to 85% at 360°C. The results are consistent with a PGM/CeO<sub>2</sub> interaction resulting in enhanced WGS activity (Diwell *et al.*, 1991). When H<sub>2</sub>O is present, CO conversion is higher. On the other hand, the water content has slightly less of an effect on the activity of Au/CeO<sub>2</sub> and moderately influenced Au/Fe<sub>2</sub>O<sub>3</sub> catalysts in the reaction temperature range of 300-360°C as illustrated in Figures 6.9 and 6.10, respectively. With 20% water content the maximum conversion increased from 8% to 15% and 33% to 53% for Au/CeO<sub>2</sub> and Au/Fe<sub>2</sub>O<sub>3</sub> catalysts, respectively.

In the literature, the water content is crucial for the activity of commercial CuO-ZnO catalysts (Gines *et al.*, 1995). The promoting effect of water vapor on Pt/CeO<sub>2</sub> can be explained as oxidation of the CeO<sub>2</sub> support by water (Holmgren *et al.*, 1999). The water in hydroxide form may play an important role as a good oxidant in WGS reaction. Holmgren *et al.* (1999), speculated that CO reacts with OH to produce CO<sub>2</sub> and H<sub>2</sub> in the WGS reaction on Pt/CeO<sub>2</sub> catalyst by using FTIR. From FTIR measurements, it was seen that Pt facilitates the formation of carbonates.

Lately, Hilaire *et al.* (2001) have shown that ceria-supported, transition metals are active catalysts for the water-gas-shift reaction. Moreover, in order to understand the mechanism for this reaction, they concluded that involves a redox process, which reduced ceria being oxidized by water and then transferring oxygen to the transition metal to react with adsorbed CO (Bunluesin *et al.*, 1998). They reported the ceria largely reduced and covered with carbonate species that may limit reaction rates.

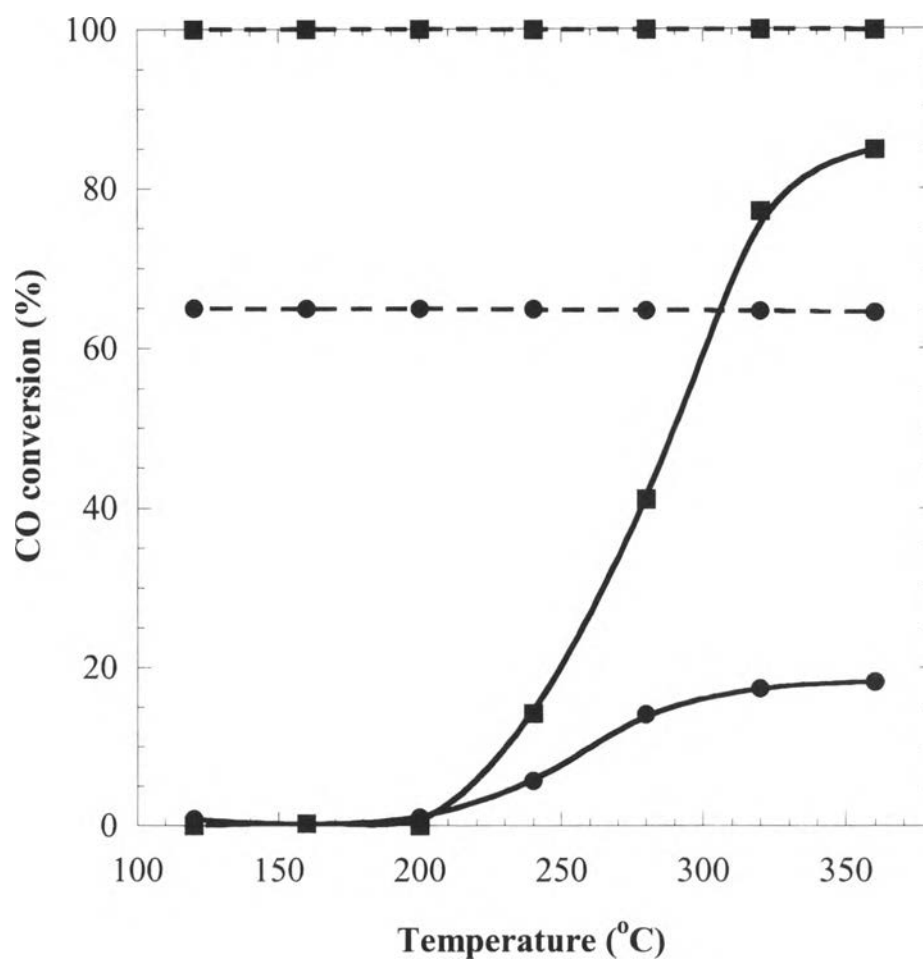


**Figure 6.8** Effect of water on catalytic activity of 1% Pt/CeO<sub>2</sub> sol-gel catalyst: (●) 2.6% water; (■) 20%water; (---) Thermodynamic equilibrium.

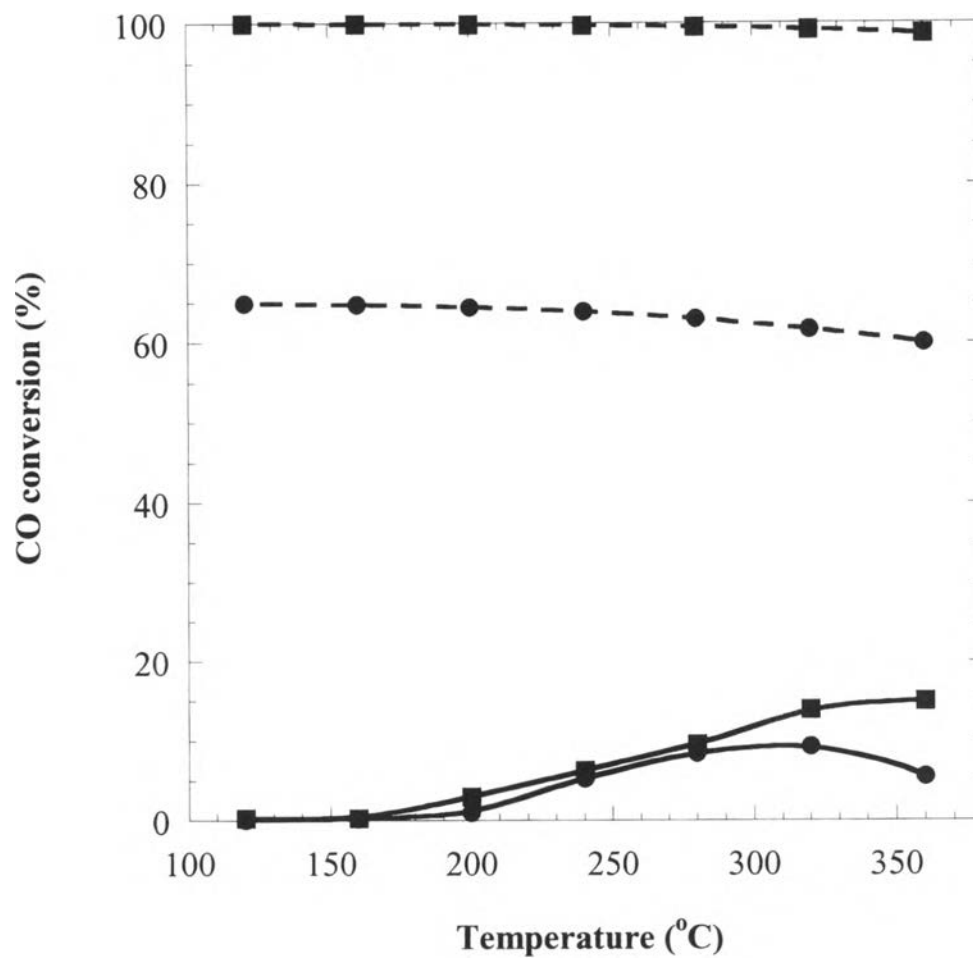


**Figure 6.9** Effect of water on catalytic activity of 1% Au/CeO<sub>2</sub> co-precipitation catalyst: (●) 2.6% water; (■) 20%water; (---) Thermodynamic equilibrium.



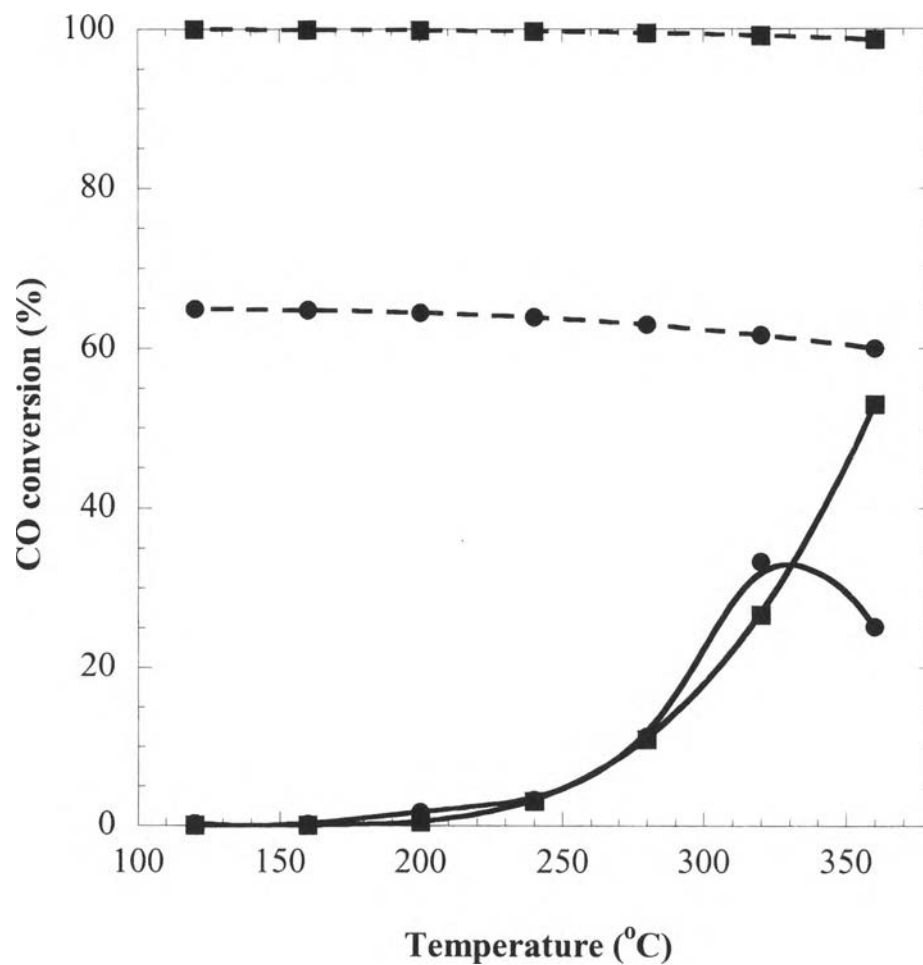


**Figure 6.10** Effect of water on catalytic activity of 3% Au/Fe<sub>2</sub>O<sub>3</sub> deposition-precipitation catalyst: (●) 2.6% water; (■) 20% water; (---) Thermodynamic equilibrium.

#### 6.2.4 Effect of Carbon Monoxide Concentration

The effect of the CO concentration on the catalytic activity of Pt/CeO<sub>2</sub> sol-gel catalyst in the WGS reaction was studied and is illustrated in Figure 6.11. In this experiment, the concentration of CO was varied from 0.5 to 2%, water concentration was 2.6% the rest being helium. As shown in Figure 6.11, there is a significant effect of CO concentration in the temperature range of 160-250°C. The activity of Pt/CeO<sub>2</sub> catalyst is in the range of 100-300°C. The differences are most distinct within the range of 160-250°C. CO conversion increases with an increase in the reaction temperature over Pt/CeO<sub>2</sub> sol-gel catalyst. However, CO conversion decreases with increasing CO concentration in the feed. At 0.5%CO in the feed, CO conversion reaches a maximum of 95% at temperature of 250°C. The decrease with increasing CO concentration is most likely due to the well-known poisoning effect of CO on Pt sites. Similar effect was also observed on Au/CeO<sub>2</sub> and Au/Fe<sub>2</sub>O<sub>3</sub> catalysts as shown on Figures 6.12-6.13.

Ovesen *et al.* (1992) assume that both the dissociation of H<sub>2</sub>O\* and the reaction between CO\* and O\* may be slow but, for large H<sub>2</sub>O/CO feed ratios, the oxidation of CO is the controlling step. In contrast to the results in the literature, Hilaire *et al.* (2001), they found the zeroth-order rate dependence for CO on Pd/CeO<sub>2</sub> for the WGS.

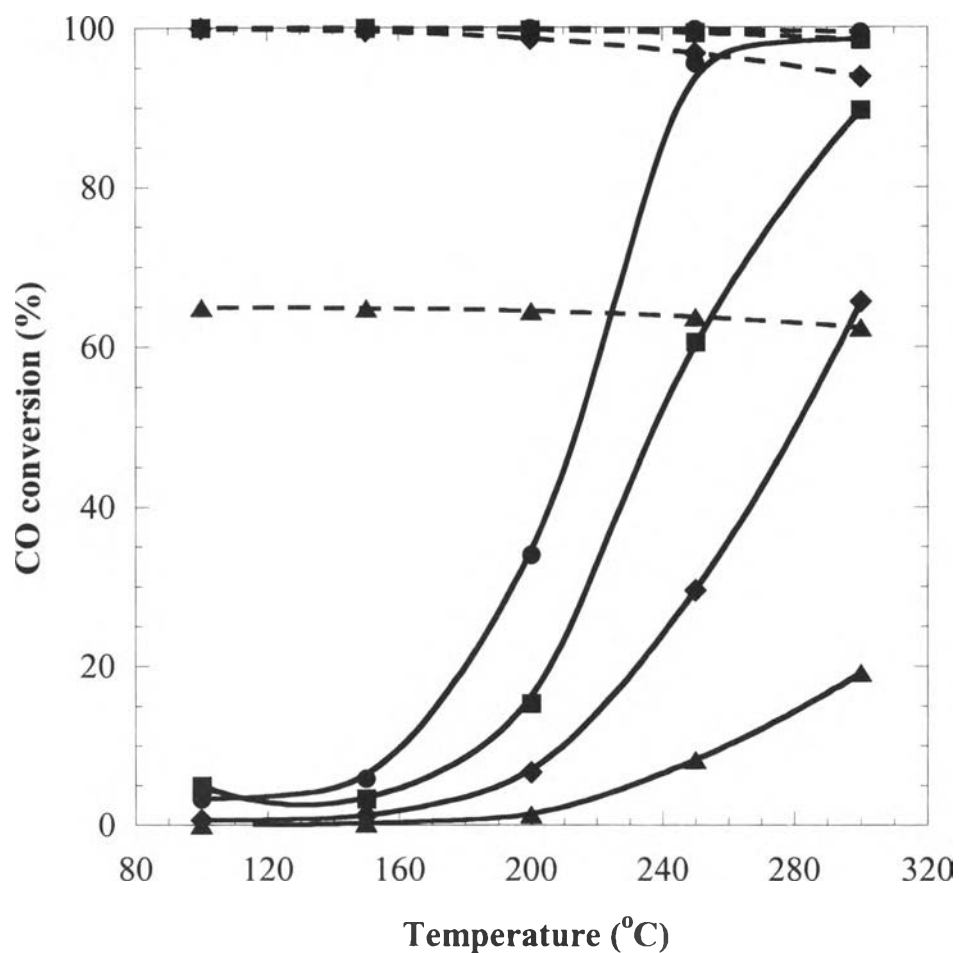


**Figure 6.11** Effect of CO on the catalytic activity of 1% Pt/CeO<sub>2</sub> sol-gel catalyst. (●) 0.5% CO; (■) 1.0%CO; (◆) 2.0%CO; (▲) 4.0%CO; (---) Thermodynamic equilibrium. Reactant composition: 0.5-4% CO, 2.6% H<sub>2</sub>O, and He.

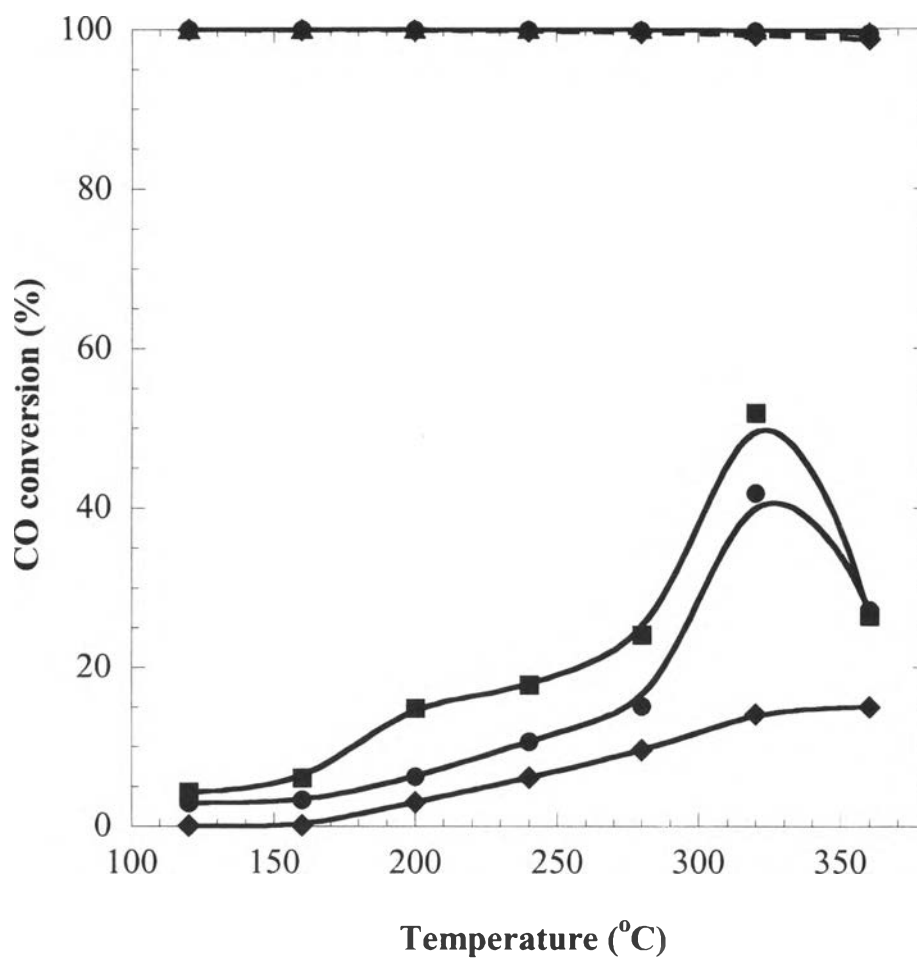


**Figure 6.12** Effect of CO on the catalytic activity of 1% Au/CeO<sub>2</sub> co-precipitation catalyst. (■) 1.0%CO; (●) 2.0% CO; (◆) 4.0%CO; (---) Thermodynamic equilibrium. Reactant composition: 1-4% CO, 20% H<sub>2</sub>O, and He.

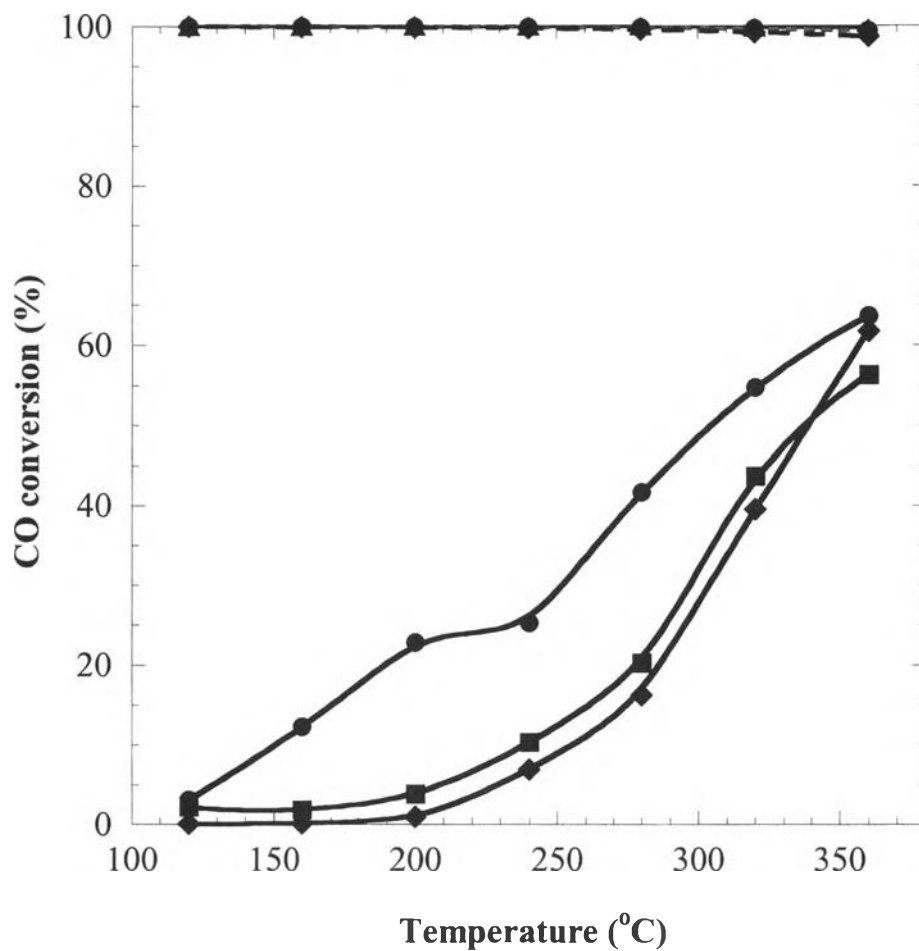


**Figure 6.13** Effect of CO on the catalytic activity of 3% Au/Fe<sub>2</sub>O<sub>3</sub> deposition-precipitation catalyst. (●) 1.0%CO; (■) 2.0% CO; (◆) 4.0%CO; (---) Thermodynamic equilibrium. Reactant composition: 1-4% CO, 20% H<sub>2</sub>O, and He.

The effect of the CO concentration on the catalytic activity of Pt/CeO<sub>2</sub>.Al<sub>2</sub>O<sub>3</sub> catalyst in the WGSR was studied and is illustrated in Figure 6.14. The concentration of CO was varied from 1 to 4%, while the water concentration was maintained at 20%. There is a significant effect of CO concentration in the temperature range of 260-360°C. The activity of Pt/CeO<sub>2</sub>.Al<sub>2</sub>O<sub>3</sub> catalyst increases with an increase in the reaction temperature, however, CO conversion decreases with increasing CO concentration. For 1%CO in the feed, CO conversion reaches a maximum of about 52% at 360°C while for 4% CO, the peak CO conversion is about 24% at the same temperature.

This result agrees with the study of the effect of CO on Pt/CeO<sub>2</sub> catalysts on WGSR. The catalytic activity increases with a decrease of CO concentration. 1% Pt/CeO<sub>2</sub>.Al<sub>2</sub>O<sub>3</sub> was substantially more active than the 1% Au/CeO<sub>2</sub>.Al<sub>2</sub>O<sub>3</sub> and 3% Au/Fe<sub>2</sub>O<sub>3</sub>.Al<sub>2</sub>O<sub>3</sub> catalysts in the presence of 20% H<sub>2</sub>O.

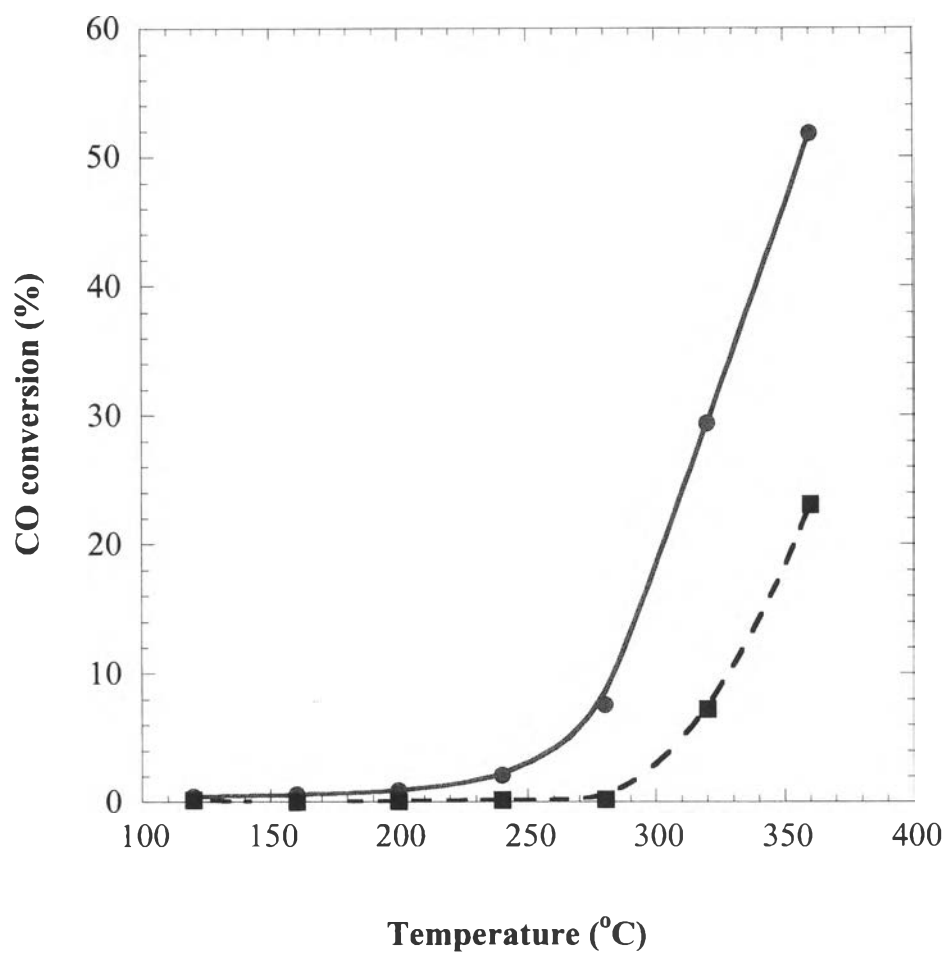


**Figure 6.14** Effect of CO on catalytic activity of 1% Pt/CeO<sub>2</sub>.Al<sub>2</sub>O<sub>3</sub> catalyst. Reactant composition: 1-4% CO, 20% H<sub>2</sub>O, 40% H<sub>2</sub> and He; (●) 1% CO; (■) 4% CO.

### 6.2.5 Deactivation Test

The catalytic stability of Pt/CeO<sub>2</sub>, Au/CeO<sub>2</sub> and Au/Fe<sub>2</sub>O<sub>3</sub> catalysts which showed the maximum activity was tested for 48 h at the temperature of 360, 360 and 320°C, respectively. The catalytic stability was carried out with a feed stream typically consisting of 2% CO, 20% H<sub>2</sub>O and helium. The result of the catalytic activity is illustrated in Figure 6.15. It is seen that Pt/CeO<sub>2</sub> catalyst showed good stability compared to the other catalysts. The stability of Au/CeO<sub>2</sub> catalyst was dramatically decreased from conversion of 60% to about 10% within 48 h. In the spent catalyst, the XRD and TEM results indicated an average size of Au catalyst was increased from 4 to 5.5 nm and this is considered to be the reason for the deactivation for the Au particles after reaction was expected because Au particles agglomerate into bigger sizes.



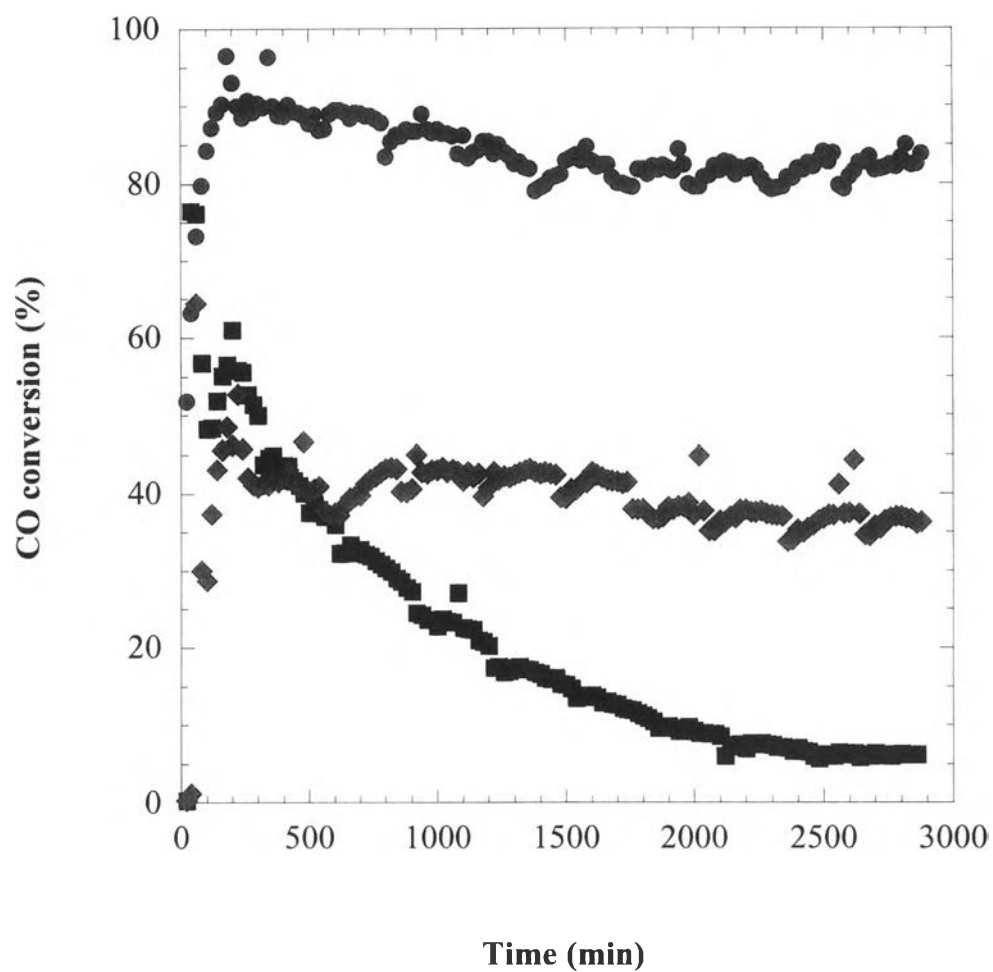


**Figure 6.15** Comparison of deactivation test of 1% Pt/CeO<sub>2</sub> sol-gel, 1% Au/CeO<sub>2</sub> co-precipitation, and 3% Au/Fe<sub>2</sub>O<sub>3</sub> deposition-precipitation catalysts. Reactant composition: 2% CO, 20% H<sub>2</sub>O and helium; (●) 1% Pt/CeO<sub>2</sub>; (■) 1% Au/CeO<sub>2</sub>; (◆) 3% Au/Fe<sub>2</sub>O<sub>3</sub>.

### 6.3 Conclusions

The catalytic activity of Pt/CeO<sub>2</sub>, Au/CeO<sub>2</sub> and Au/Fe<sub>2</sub>O<sub>3</sub> catalysts has been investigated for low temperature WGS reaction. We find that the crystallinity of the reducible oxide support negatively affects the activity of the catalyst. The activity of metal/cerium oxide catalysts strongly depends on type of metal with Pt being a much more active catalyst than Au. These findings indicate that Pt as well as CeO<sub>2</sub> plays an important role in this reaction. We also observed that water had a positive effect on the Pt/CeO<sub>2</sub> catalyst and a moderate positive effect on the Au/CeO<sub>2</sub> and Au/Fe<sub>2</sub>O<sub>3</sub> catalysts. In addition, it was found that CO concentration greatly affected the activity of Pt/CeO<sub>2</sub>, Au/CeO<sub>2</sub> and Au/Fe<sub>2</sub>O<sub>3</sub> catalysts.

Our investigations on gold-based catalytic systems clearly demonstrated the Fe<sub>2</sub>O<sub>3</sub> is not the most suitable supports for WGS reaction which was found by Andreeva *et al.* (1996) and Andreeva *et al.* (1998). The catalytic activity and stability tests show that activity of the gold-containing catalysts is decreasing during the catalytic tests. The effect of addition of about 40% of H<sub>2</sub> into the gas mixture was also examined. A low WGS activity in the presence of H<sub>2</sub> is also exhibited by the Au-containing catalysts. The increased activity and stability by the modification of Fe<sub>2</sub>O<sub>3</sub> or CeO<sub>2</sub> with high surface area of Al<sub>2</sub>O<sub>3</sub> for this reaction was not achieved. Accordingly, the Pt supported on CeO<sub>2</sub> catalysts seemed to be appropriate for the WGS reaction at moderate reaction conditions and high H<sub>2</sub>O/CO in comparison with the Au catalysts in the presence and absence of H<sub>2</sub>.